WORLD CONFERENCE ON TIMBER ENGINEERING 2025
BRISBANE, AUSTRALIA
Advancing Timber for the Future Built Environment

# EFFECT OF BRACING IRREGULARITY ON SEISMIC PERFORMANCE OF L-SHAPED LIGHT TIMBER-FRAMED RESIDENTIAL HOUSES

Kexin Wang[1], Minghao Li [2], Angela Liu [3], Rajesh P. Dhakal[4]

**ABSTRACT:** Lessons from previous earthquakes indicate that light timber-framed (LTF) residential houses are at high risk of suffering severe damage in major earthquakes. The bracing irregularity is one of the essential factors affecting the seismic performance of the entire structure, and the current design standard in New Zealand NZS3604 specifies several limits to ensure that the bracing elements are evenly distributed along bracing lines. However, the effect of bracing irregularity is likely to be greater in L-shaped structures and there is no specific irregularity limit for L-shaped LTF houses. The aim of this paper is to quantify the effect of bracing irregularity on seismic performance of L-shaped LTF residential houses. Three single-storey L-shaped LTF case study houses in New Zealand with different irregularity levels were selected and modelled. Incremental dynamic analyses (IDA) were then conducted for these cases study structures. The simulation results showed that the L-shaped house with bracing arrangements permitted by the irregularity limits of NZS3604 had much greater inter-storey drift ratios and significant torsion in earthquakes than the regularly braced house.

**KEYWORDS:** light timber-framed structure, bracing irregularity, seismic performance, plasterboard bracing wall

## 1 – INTRODUCTION

Low-rise light timber-framed (LTF) structures normally have a low probability of collapse under earthquakes. Previous research [1,2] concluded that low-rise LTF houses could sustain a storey drift of 6% before reaching the collapse limit state. Past earthquake experiences also indicate that LTF residential housing stocks generally perform well to meet the life safety performance target. However, LTF residential houses could suffer significant damage in major earthquakes, leading to significant downtime and economic losses for the community. As an example, the post-earthquake survey of 2011 Mw6.3 Christchurch earthquake reported that cracks in plasterboard and even plasterboard detachments were observed in many LTF residential houses [1]. The estimated total economic losses of residential houses caused by the 2010-11 Canterbury earthquake sequence were around $12B, about 30% of the total losses [3].

The bracing irregularity is an essential factor that effects the seismic performance and damage of LTF residential houses. In LTF residential houses, shear walls provide a large proportion of the stiffness and resistance to lateral wind and seismic loads. Generally, the bracing irregularity of LTF residential houses is caused by uneven arrangement of shear walls. The current design standard in New Zealand specifies bracing arrangement limits to ensure that the shear walls are relatively evenly distributed along bracing lines. However, the effect of bracing irregularity is likely to be greater in structures with wings, such as L-shaped, U-shaped and T-shaped structures. A post-earthquake damage survey [4] of the 2010 Mw7.1 Darfield earthquake found that L- shaped and U-shaped LTF houses suffered greater damage at the intersection of the wings.

Residential houses with wings are widely constructed, due to benefits such as efficient utilization of interior space, natural light, privacy, and indoor-outdoor harmony. These houses are considered as exhibiting geometric irregularities. If the distribution of shear walls in a structure with wings is not uniform, i.e., it has both geometry irregularity and bracing irregularity, the

[1] Kexin Wang, Department Civil and Natural Resources Engineering, University of Canterbury, Christchurch, New Zealand, kexin.wang@pg.canterbury.ac.nz

[2] Minghao Li, Department of Wood Science, University of British Columbia, Vancouver, Canada, minghao.li@ubc.ca

[3] Angela Liu, BRANZ Ltd, Porirua, New Zealand, angela.liu@branz.co.nz

[4] Rajesh P. Dhakal, Department Civil and Natural Resources Engineering, University of Canterbury, Christchurch, New Zealand, rajesh.dhakal@canterbury.ac.nz

https://doi.org/10.52202/080513-0176

seismic performance of such a house will be greatly compromised. Nonetheless, few studies have analysed the effect of bracing irregularity on seismic performance of LTF residential houses with wings.

In New Zealand, for example, most residential houses are low-rise LTF houses and over 90% of them adopt plasterboard bracing wall systems. Compared with LTF walls sheathed by plywood and OSB, plasterboard bracing walls have lower ductility, lower strength, lower energy dissipation, and smaller ultimate displacement [5,6]. As per the New Zealand standard for timber-framed buildings NZS3604[7], the bracing walls must meet the bracing demand and be evenly distributed along notional bracing lines in two orthogonal directions of the building. But there is no specific irregularity limit for LTF houses with wings. Specific provisions for bracing wall arrangements in NZS3604 include:

- The bracing lines in any storey shall be placed at not more than 6 m centres apart;
- On each bracing line, the minimum bracing provision is the greater of 100 BUs (bracing units, where 1 kN equals 20 BUs) or 50% of the total bracing demand divided by the number of bracing lines in the direction being considered;
- The minimum bracing resistance for each external wall in any storey shall be no less than 15 BUs/m of the external wall length.

This study focuses on L-shaped LTF residential houses, aiming to quantify the effect of bracing irregularity on their seismic performance. Three single-storey L-shaped LTF houses with different irregularity levels were selected for the cases study. 3D numerical models were built for these three structures. Incremental dynamic analyses (IDA) were then conducted to assess their seismic performance under earthquakes of different magnitudes. The effect of bracing irregularity in L-shaped LTF residential houses was analysed in terms of overall structure performance, torsions, maximum roof drifts and relative displacements between substructures.

## 2 – CASE STUDY STRUCTURES

Three case study structures were selected from a BRANZ study [8], which were designed per New Zealand standard for timber-framed buildings NZS3604. These three structures are all one-storey LTF structures and share the same outlines. As shown in Figure 1, these structures have an “L” shaped outline with an overall length of 16 m and a width of 11 m, which are common dimensions for single-family houses. In the design of these structures, they were assumed to be constructed on a site with a seismic hazard factor of Z = 0.46 and subsoil class D according to the New Zealand standard of design earthquake actions NZS 1170.5 [9]. They all have reinforced concrete ribbed slab foundations, corrugated metal roofs and heavy wall cladding. The roof pitch is less than 25° and the storey height is 2.4 m. The total seismic mass is 13,305 kg, including the dead and live load. The average mass is 114.70 kg/m$^2$, assuming that the mass is uniformly distributed over the floor area of 116 m$^2$.

According to NZS1170.5, the earthquake bracing demand is developed based on the force-based equivalent static method. The design base shear force, $V$, is determined by the following equation:

$$V = C_d(T_1)W_t \quad (1)$$

where $C_d(T_1)$ is the horizontal design action coefficient derived by assuming a ductility of $\mu$ and a fundamental period of $T_1$, and $W_t$ is the seismic weight. For light-timber structures, the ductility factor $\mu$=3.5 and the fundamental period $T_1$=0.4 s, according to NZS3604. According to equation 3.1 and 5.1 in NZS1170.5, the horizontal design action coefficient of these three structures $C_d(T_1)$=0.4. Therefore, the total seismic demand for the whole structure is about 1044 BUs (=52.2 kN) and the average seismic demand is 9 BUs/m$^2$ (=0.45 kN/m$^2$). The bracing walls in these structures are all plasterboard bracing walls. The extra bracing walls lined by standard plasterboards on the inside face and have no hold-downs, marked by PLW1 in this study. The internal bracing walls lined by standard plasterboards on both faces and have no hold-downs, marked by PLW2. The bracing ratings are 60 BUs for PLW1 and 80 BUs for PLW2.

The only difference between these three structures is the arrangements of bracing walls across the floor plan. The first structure is regular in the X and Y directions, named LR. The second is irregular in the Y direction only, named LIR1, and the third is irregular in both directions, named LIR2. Figure 1 illustrates the bracing wall arrangements of the three case study structures, and the wall types and lengths are marked. The bracing designs are shown in Table 1. The bracing arrangements of LIR1 and LIR2 are close to the allowable irregularity limit in NZS 3604. Here, the allowable irregularity limit refers to the bracing capacity of the edge wing line of the wing reaches 50% of the total bracing demand of the wing divided by the number of bracing lines in the considered direction. Taking Line 4 as an example, the limit is equal to 50 % of the bracing demand for the wing area between Line 2 and Line 4 divided by number of bracing lines in this wing, i.e. 50%×450BUs/3=75 BUs. In house LIR1


https://doi.org/10.52202/080513-0176

and LIR2, the bracing capacity of Line 4 is designed as 75 BUs.

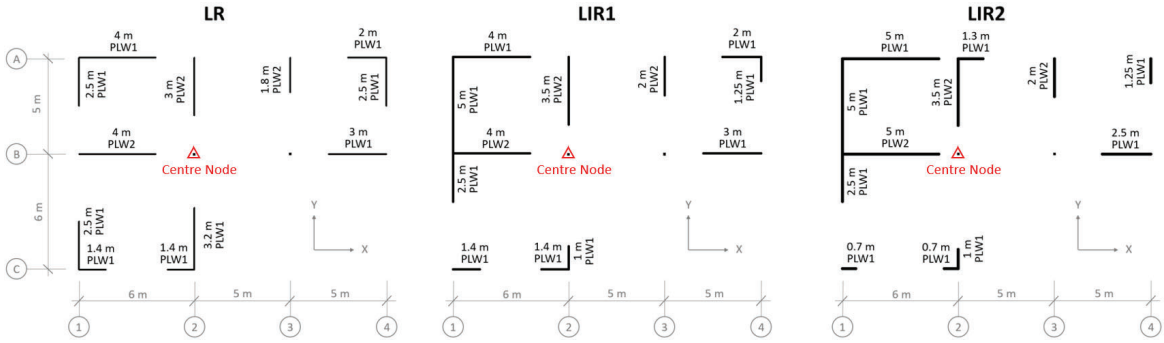


*Figure 1. Bracing arrangements of three case study structures.*

*Table 1: Summary of bracing designs of three case study structures*

| | | X direction | | | Y direction | | | |
|---|---|---|---|---|---|---|---|---|
| Bracing line number | | A | B | C | 1 | 2 | 3 | 4 |
| Total bracing demand (BUs) | | 1044 | | | 1044 | | | |
| LR | Bracing provision (BUs) | 360 | 520 | 168 | 300 | 447 | 153 | 150 |
| | Total bracing provision (BUs) | 1048 | | | 1050 | | | |
| LIR1 | Bracing provision (BUs) | 360 | 520 | 168 | 450 | 358 | 170 | 75 |
| | Total bracing provision (BUs) | 1048 | | | 1053 | | | |
| LIR2 | Bracing provision (BUs) | 378 | 596 | 90 | 450 | 358 | 170 | 75 |
| | Total bracing provision (BUs) | 1064 | | | 1053 | | | |

## 3 – NUMERICAL MODELLING

This study uses a computer-based structural analysis tool called "PB3D" for modelling the case study structures. This three-dimensional analysis platform was developed by Li et al. [10] to perform nonlinear time history analysis of residential post and beam timber buildings under seismic loads. In this platform, the diaphragms are modelled by beam elements and diagonal truss elements considering the in-plane stiffness, and beams and posts are modelled by elastic beam elements. The shear walls are modelled by a macro model which was derived by a mechanics-based model named "pseudo-nail" model. The uplifting is simply prevented by wall post elements which are fully end-restrained onto the foundation or stories. Fig. 2 shows the schematics of a PB3D model. For these case study structures, the damping ratio was assumed as 5%.

The "pseudo-nail" model is a typical macro wall model revised from a nail connection model named HYST [11], because the global hysteretic behaviour of LTF shear walls is similar to that of nail-to-wood connections. HYST is a common panel-frame nail connection model used in wood shear walls. A modified HYST algorithm, developed by Li et al. [12], improved the computational efficiency and addressed the stiffness degradation effect. Fig. 3 illustrates the schematics of HYST panel-frame nailed connection. The parameters in this model include the nail length L, nail diameter D, and six parameters to describe the compressive properties of the surrounding embedment medium. These parameters can be calibrated by shear wall test data or detailed wall models.

A series of "pseudo-nail" models were developed by Wang et al. [6] for plasterboard bracing walls used in New Zealand based on experimental results, including PLW1 and PLW2 walls using in the case study structures of this study. The overall model predictions agreed well with the test results in terms of the maximum load at each displacement level, pinching strength degradation and energy dissipation. Using 1.2 m long PLW1 wall (a bracing wall lined by standard plasterboards on the inside face only and have no hold-downs) as an example, the hysteretic load-drift curves of the test and the "pseudo-nail" model predications are illustrated in Fig. 4. It shows that this model predicts the hysteretic behaviour very well.

The timber diaphragm of each room is modelled by a pair of diagonal truss elements based on the equivalent truss

https://doi.org/10.52202/080513-0176

method developed by Moroder [13]. With this method, the diagonal trusses can present the shear stiffness and fastener flexibility, characterized by the following properties:

$$(Gd)_{ef} = \frac{1}{\frac{1}{Gd} + \frac{s}{K_{ser\|}}\left(\frac{c_1}{b} + \frac{c_2}{h}\right)} \quad (2.1)$$

$$E_{ef} = \frac{(Gd)_{ef}\, l^2}{hb} \quad (2.2)$$

$$A_{ef} = l = \sqrt{h^2 + b^2} \quad (2.3)$$

where $(Gd)_{ef}$ is the equivalent shear-through-thickness rigidity of the panel, $G$ is the shear modulus of the sheathing, $d$ is the sheathing panel thickness, $E_{ef}$ is the equivalent modulus of elasticity of the diagonal truss, $A_{ef}$ is the equivalent cross sectional area of the diagonal truss, $K_{ser\|}$ is slip modulus of the fastener parallel to the panel edge, $s$ is the fastener spacing, $b$ and $h$ are the panel's width and height, $l$ is length of the diagonal truss, and $c_i$ is the number of connections rows along sheathing panel edge, taking 2 for nailed light timber diaphragms. Fig. 5 shows the schematics of a quadrilateral system with a pair of equivalent diagonal trusses.

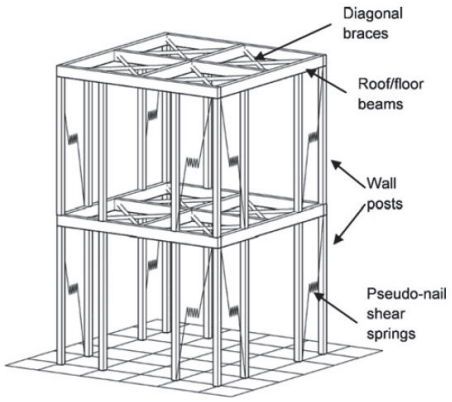


*Figure 2. Schematics of a "PB3D" model* [10].

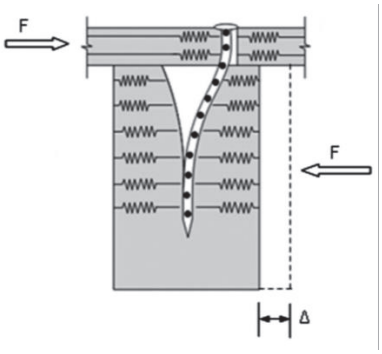


*Figure 3. Schematics of HYST panel-frame nailed connection* [12].

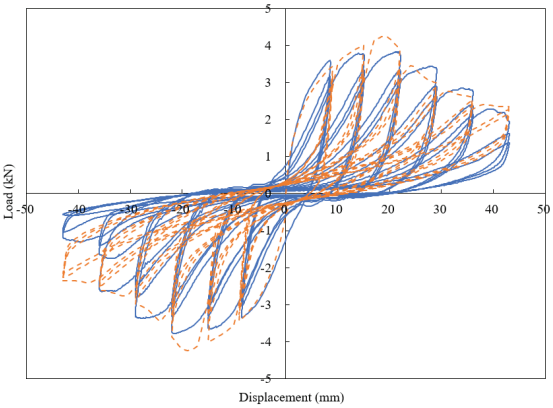


*Figure 4. Hysteretic load-drift curves of test result and "pseudo-nail" model for 1.2m long PLW1 wall.*

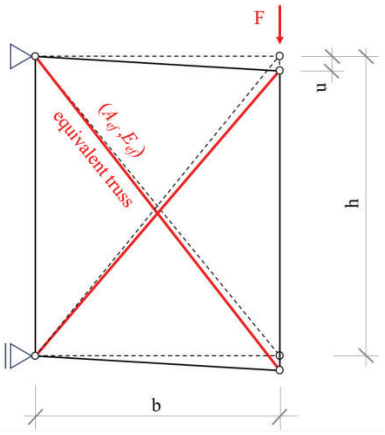


*Figure 5. Schematics of a quadrilateral system with a pair of equivalent diagonal trusses (edited from [13]).*

## 3 – SIMULATION ANALYSIS

### 3.1 INCREMENTAL DYNAMIC ANALYSIS

To assess the seismic performance of these three L-shaped case study structures, incremental dynamic analysis (IDA) was conducted. IDA is a common method for assessing the global capacity of a component/structure under seismic loading [14]. The main aims include a better understanding of the changes in the nature of the structural response as the intensity of ground motion increases, and the differences in structural performance across different ground motion records. Performing an IDA requires the following steps: 1) choosing suitable ground motion intensity measures (IM) and representative damage measures (DM); 2) selecting a suite of ground motion records; 3) for each record, incrementally scale it to multiple IM levels and run a nonlinear dynamic analysis; 4) postprocessing the results of the dynamic analyses, i.e.


https://doi.org/10.52202/080513-0176

interpolating the resulting IM, DM points to generate an IDA curve for each record [15,16].

In this study, the 5%-damped spectral acceleration response at the fundamental period of the structure, i.e., Sa($T_1$), was used as the scaled intensity measure. The determination of the fundamental periods of the case study structures ($T_1$) was introduced in the following section. The damage measure took the roof drift ratio, because the main seismic damage to low-rise LTF structures is normally caused by the inter-storey drift ratios of bracing walls. A ground motion set of New Zealand records was selected for IDA, including 20 ground motion records of 2010-2011 canterbury earthquake and 2016 Kaikōura earthquake. The detailed information of these records is shown in Table 2. Fig. 6 shows the 5%-damped spectrums of all records. When scaling these ground motion records to different intensity levels, the scaled factors were limited in the range from 0.33 to 3 to avoid introducing bias in the response estimation.

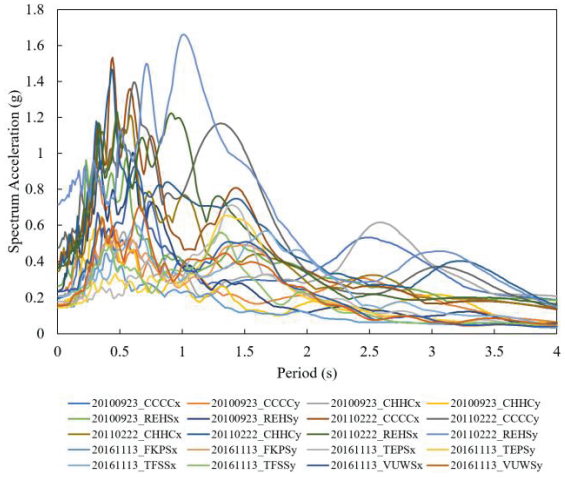


*Figure 6. Spectrums of ground motion records for IDA.*

## 3.2 DETERMINATION OF THE FUNDAMENTAL PERIOD

In this study, the fundamental periods of the case study structures were determined based on the fact that the frequency response function of a structure would experience maximum amplification around the modal frequencies of the testing structure [17]. This method is also widely used for testing real structures, so called the ambient vibration test/method [18,19]. The general process of this method for determining the fundamental periods is as follows: 1) exciting the structure using an external random signal (e.g. stationary Gaussian white noise), 2) recording the key acceleration history on the structure roof, 3) conducting a fast Fourier transform (FFT) for the acceleration record to get the Fourier spectrum, 4) determine the frequency of the peak spectrum magnitude ($f_{max\ magnitude}$), and then $T_1 = f_{max\ magnitude}$. For the case study structures in this study, the external acceleration excitation took a randomly generated Gaussian white noise with an amplitude of 0.05g. The structures were tested in the X and Y direction individually. The intersection of Line 2 and Line B on roof was taken as the acceleration recording point, because the point is the closest to the mass centre of the L-shape and can roughly present the behaviour of the whole roof. This point is marked as "centre node" in Fig 1.

Fig. 7 shows an example of the result FFT spectrum for the structure LR in the X direction. The spectrum magnitude reached the peak at 7.251 Hz, therefore, $T_1$ is equal to 1/7.251=0.138s. The fundamental period results of the three case study structures are summarised in Table 3. Comparing the $T_1$ of structures with different bracing irregularity levels shows that the fundamental period of the structure is slightly increased by the bracing irregularity. In the end, 0.15s was estimated to be the fundamental period of all these three structures.

It is noted that the value of $T_1$ determined here (around 0.15s) is lower than $T_1$ used in the bracing design of these case study structures (0.4s). In fact, $T_1$=0.4s is a general assumption for designing LTF structures according to NZS3604. Some other research [39,40,43] have also stated that the design assumption of $T_1$ is larger than that of the actual low-rise LTF residential houses. However, when designing in accordance with the equivalent static method in NZS 1170.5, the horizontal design action coefficient $C_d(T_1)$ remains constant over a range of $T_1$ of 0 to 0.4s. Therefore, using the design assumption of $T_1$=0.4s does not affect the design base shear forces of these structures.

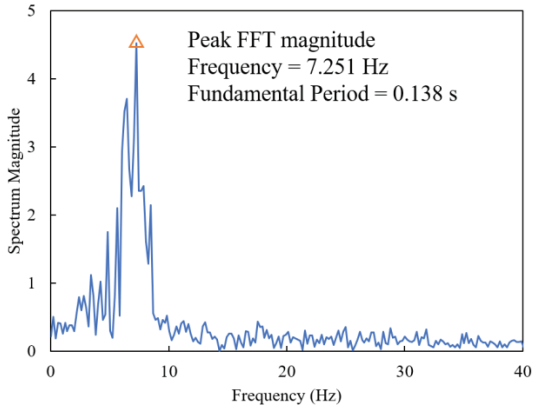


*Figure 7. FFT spectrum of the roof acceleration history in the structure LR in the X direction exciting by a Gaussian white noise.*

https://doi.org/10.52202/080513-0176

*Table 3: The fundamental period results of the three case study structures (s).*

| | X direction | Y direction |
|---|---|---|
| LR | 0.138 | 0.155 |
| LIR1 | 0.138 | 0.177 |
| LIR2 | 0.155 | 0.177 |

# 4 – RESULTS

## 4.1 RESPONSES AT ROOF CENTRE

The drift ratio of the roof centre node (marked in Fig.1) was used to represent the overall structure performance. IDA curves were generated by interpolating the IDA resulting points of drifts verves $Sa(T_1)$ for all ground motion records. Since the structures were tested in the X and Y direction individually, the IDA curves were plotted separately for two directions, as shown in Fig. 8(a) and (b).

As shown in these two figures, there exists variations in the seismic performance for various intensity levels of ground motion records. This type of variations can be well described by the lognormal distribution, which was concluded by various studies (e.g. [20,21]), i.e.

$$\ln X \sim N(\theta, \beta^2) \tag{3.1}$$

$$\theta = \mu_{\ln X} \tag{3.2}$$

$$\beta^2 = \sigma^2_{\ln X} = \ln\left(\left[\frac{\sigma_X}{\mu_X}\right]^2 + 1\right) \tag{3.3}$$

where the variable $X$ represents *Drift|IM=im*, the peak roof drift under earthquakes of the *im* intensity measure level; $\theta$ and $\beta$ are the mean and standard deviation of $ln\ X$; $\mu_X$ and $\sigma_X$ are the mean and standard deviation of the variable $X$. $\beta$, also called the dispersion, can be used to quantify the uncertainty of the seismic performance caused by the uncertainty of ground motion records with the same intensity level. The $\beta$ values for IDA curves of the overall performance of the structures are illustrated in Fig. 8(a) and (b). It shows that the dispersions are acceptable, all under 0.6.

*Table 2: Information of the ground motion set for IDA*

| No. | Event | Date | Component | Station | $Sa(T_1)$ (g) |
|---|---|---|---|---|---|
| 1 | 2010 Canterbury | 23/09/2010 | EW | Christchurch Cathedral College (CCCC) | 0.3263 |
| 2 | 2010 Canterbury | 23/09/2010 | NS | Christchurch Cathedral College (CCCC) | 0.4260 |
| 3 | 2010 Canterbury | 23/09/2010 | EW | Christchurch Hospital (CHHC) | 0.2439 |
| 4 | 2010 Canterbury | 23/09/2010 | NS | Christchurch Hospital (CHHC) | 0.2326 |
| 5 | 2010 Canterbury | 23/09/2010 | EW | Christchurch Resthaven (REHS) | 0.4350 |
| 6 | 2010 Canterbury | 23/09/2010 | NS | Christchurch Resthaven (REHS) | 0.4591 |
| 7 | 2011 Canterbury | 22/02/2011 | EW | Christchurch Cathedral College (CCCC) | 0.5177 |
| 8 | 2011 Canterbury | 22/02/2011 | NS | Christchurch Cathedral College (CCCC) | 0.5763 |
| 9 | 2011 Canterbury | 22/02/2011 | EW | Christchurch Hospital (CHHC) | 0.5141 |
| 10 | 2011 Canterbury | 22/02/2011 | NS | Christchurch Hospital (CHHC) | 0.5273 |
| 11 | 2011 Canterbury | 22/02/2011 | EW | Christchurch Resthaven (REHS) | 0.5246 |
| 12 | 2011 Canterbury | 22/02/2011 | NS | Christchurch Resthaven (REHS) | 0.8548 |
| 13 | 2016 Kaikōura | 13/11/2016 | EW | Wellington Frank Kitts Park (FKPS) | 0.1866 |
| 14 | 2016 Kaikōura | 13/11/2016 | NS | Wellington Frank Kitts Park FKPS | 0.1872 |
| 15 | 2016 Kaikōura | 13/11/2016 | EW | Wellington Te Papa Museum TEPS | 0.1762 |
| 16 | 2016 Kaikōura | 13/11/2016 | NS | Wellington Te Papa Museum TEPS | 0.1632 |
| 17 | 2016 Kaikōura | 13/11/2016 | EW | Wellington Thorndon Fire Station TFSS | 0.2418 |
| 18 | 2016 Kaikōura | 13/11/2016 | NS | Wellington Thorndon Fire Station TFSS | 0.2259 |
| 19 | 2016 Kaikōura | 13/11/2016 | EW | Victoria University Law School VUWS | 0.2461 |
| 20 | 2016 Kaikōura | 13/11/2016 | NS | Victoria University Law School VUWS | 0.2225 |


https://doi.org/10.52202/080513-0176

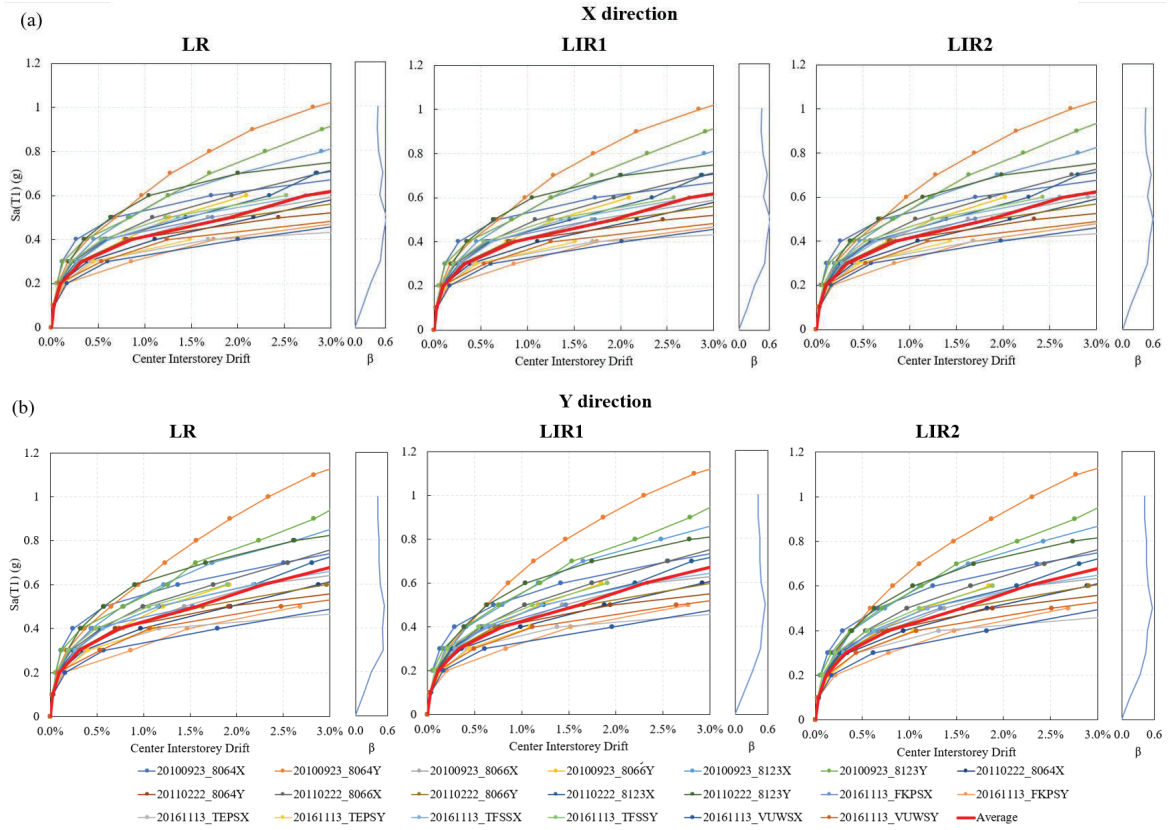


*Figure 8. IDA curves of roof centre drift ratio:(a) X direction, (b) Y direction.*

Each red line in Fig. 8(a) and (b) is the mean curve of all IDA curves of that scenario. It shows that, in each direction, the mean IDA curves of house LR, LIR1 and LIR2 are almost overlapping. This means that the drift ratios of the roof centre are not affected by the bracing irregularity in L-shaped LTF houses. In fact, the bracing irregularity can cause a torsion to the roof diaphragm and the maximum drift of the roof would be larger than the drift of the roof centre. Therefore, if only focusing on drifts of the roof centre, the performance of L-shaped LTF houses would be over estimated and the effect of the bracing irregularity would be ignored.

## 4.2 TORSIONAL RESPONSES

The torsional responses of the roof diaphragm can be calculated as the relative drift between two edge lines divided by the distance between these two edges lines. The torsion of the X and Y direction are calculated as follows:

$$Torsion\ X = \frac{|Drift\ of\ Line\ A - Drift\ of\ Line\ C|}{Distance\ between\ Line\ A\ and\ C} \quad (4.1)$$

$$Torsion\ Y = \frac{|Drift\ of\ Line\ 1 - Drift\ of\ Line\ 4|}{Distance\ between\ Line\ 1\ and\ 4} \quad (4.2)$$

Then IDA curves of the torsion versus Sa($T_1$) were generated for the three case study structures, as shown in Fig.9. The result shows that torsions increased with increasing Sa($T_1$) and had acceptable variations among different ground motion records, all lower than 0.5. House LR, the one with regular bracing plan, performed well with no apparent torsion. House LIR1, the one with irregular bracing plan in the Y direction only, had much larger torsions in the Y direction than house LR but had small torsions in the X direction. House LIR2, the one with irregular bracing plan in both directions, had larger torsion in the X and Y direction than house LIR1. Under earthquakes of the design intensity level, Sa($T_1$) = 0.4g, the torsions of house LR, LIR1 and LIR2 were 5E-5, 7.2E-4, 9.9E-4 in the Y direction, and 2E-5, 3E-5, 2.4E-4 in the X direction, respectively.

https://doi.org/10.52202/080513-0176

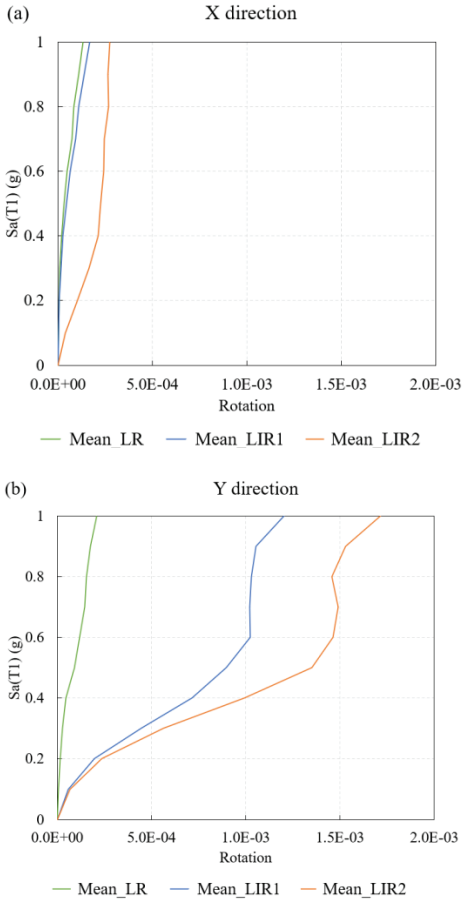


*Figure 9. Mean curves of torsions versus Sa($T_1$) for house LR, LIR1 and LIR2: (a) X direction; (b) Y direction.*

## 4.3 MAXIMUM ROOF DRIFTS

In the LTF residential houses with irregular bracing arrangements, the bracing lines with lower bracing capacities would have larger inter-storey drifts. The maximum roof drifts can represent the worst wall performance of the whole structure. The IDA curves were redrawn by taking the maximum roof drifts as the representative damage measures. The results show that dispersions of IDA curves for the three case study structures were all lower than 0.6. For brevity, only the mean IDA curves of the three case study structures (which represent the average performance) are presented in Fig. 10.

As can be seen in the comparison, in the X direction, the mean curves of these three structures were close but the maximum drifts of house LIR2 were slightly larger than these of house LR and LIR1. That is because the width of house LIR2 in the X direction was relatively short and the effect of the bracing irregularity was not too large. As shown in the last section, the torsion of house LIR2 in the X direction was also not large. In the Y direction, the maximum drifts of house LIR1 and LIR2 were much larger than these of house LR. Under earthquakes of the design intensity level, Sa($T_1$) = 0.4g, the maximum drifts of house LIR1 and LIR2 were 1.05% and 1.15%, about 1.5 times of that of house LR.

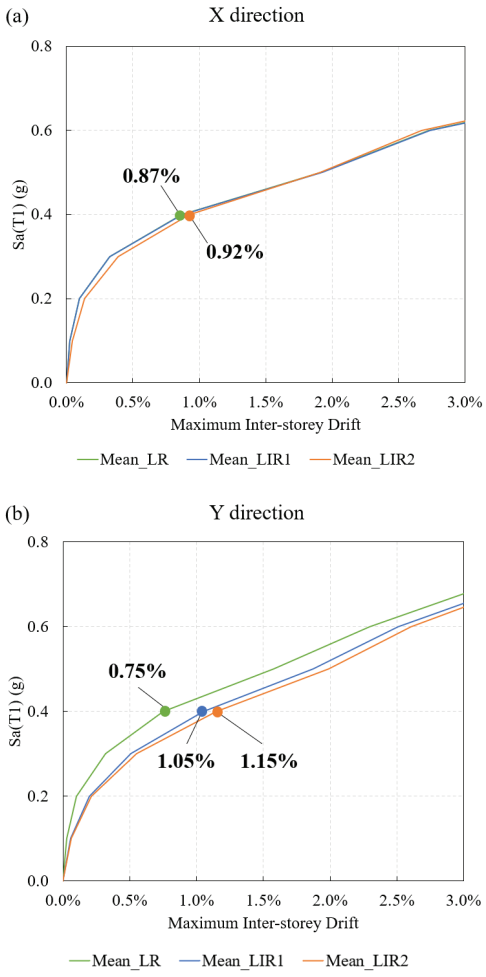


*Figure 10. Mean curves of maximum drift versus Sa($T_1$) for house LR, LIR1 and LIR2: (a) X direction; (b) Y direction.*

## 4.4 RELATIVE DISPLACEMENT BETWEEN SUBSTRUCTURES

One more performance measure used in the study was the relative displacement between substructures. In the L-shaped LTF residential houses with irregular bracing arrangements, the wing and the main structure would have out-of-sync drifts and the relative displacement between these two substructures would be larger than of the regular braced L-shaped LTF house and this may affect the performance of the roof diaphragm.

Using the structure excited in the Y direction as an example, the relative displacement of the two substructures is equal to the absolute value of difference


https://doi.org/10.52202/080513-0176

between the displacements of Line 2 and 3. IDA curves were generated for these case study structures by taking the points of the relative displacements versus $Sa(T_1)$. The results showed that the dispersions of most intensity levels were lower than 0.6, so here we also only compared the mean IDA curves of house LR, LIR1 and LIR2, as illustrated in Fig. 11. The overall trend was that the relative displacement between substructures increased with increasing $Sa(T_1)$. Houses LIR1 and LIR2 had much larger relative displacements between substructures than the house LR. Under earthquakes of the design intensity level, $Sa(T_1)$ = 0.4g, the relative displacements in house LIR1 and LIR2 were 3.73mm and 4.85mm, respectively. However, these values were not significant for the roof diaphragm of the affected area (5m in width). The horizontal drifts of the roof diaphragm for house LIR1 and LIR2, equal to the relative displacement divided by the width of the diaphragm, were 0.07% and 0.10%, respectively.

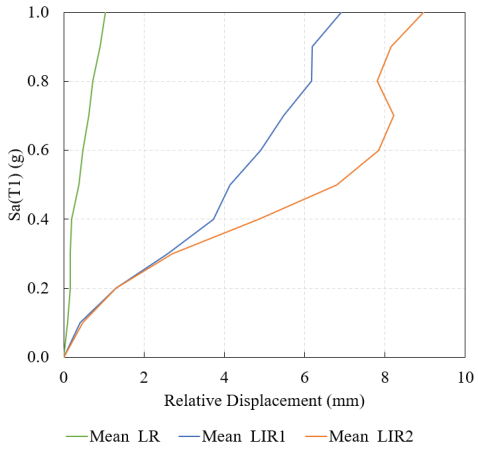


*Figure 11. Mean curves of relative displacement of wings versus $Sa(T_1)$ for house LR, LIR1 and LIR2 (Y direction).*

## 5 – CONCLUSIONs

In this paper, three single-storey L-shaped LTF cases study houses representative of houses commonly built in New Zealand with different irregularity levels were selected and modelled. Incremental dynamic analyses (IDA) were then conducted for these cases study structures to assess their seismic performance. The main findings of this paper are listed as follows:

(1) For the L-shaped LTF residential houses, the effect of the bracing irregularity would not significantly affect the response of the roof centre.

(2) The regularly braced L-shaped LTF house performed well with no apparent torsional effect detected.

(3) Compared with the regularly braced house, the L-shaped LTF house with irregular bracing arrangements testing the allowable irregularity limits in NZS3604 had much greater inter-storey drift ratios and significant torsions. Under earthquakes of the design intensity level, the irregularity of L-shaped houses has been shown to cause torsions in excess of 7E-4, and maximum drifts in excess of 1%, approximately 1.5 times of that of regularly braced L-shaped houses. The bracing walls in irregularly braced L-shaped houses are more likely to reach their drift limits.

(4) The bracing irregularity of L-shaped LTF houses can increase the relative displacement between substructures (the main structure and the wing), but the drift ratios of the roof diaphragm are all lower than 0.1%.

## 6 – REFERENCES

[1] A. Buchanan, D. Carradine, G. Beattie and H. Morris. “Performance of Houses during the Christchurch Earthquake of 22 February 2011”. In: Bulletin of the New Zealand Society for Earthquake Engineering, 44.4 (2011), pp. 342–357.

[2] P. Paevere, G. Foliente and B. Kasal. “Load-Sharing and Redistribution in a One-Story Woodframe Building”. In: Journal of Structural Engineering, 129.9 (2003), pp. 1275–1284.

[3] N. Horspool, A. King, S. Lin and S. Uma. “Damage and Losses to Residential Buildings during the Canterbury Earthquake Sequence”. In: 2016 New Zealand Society for Earthquake Engineering Conference, Christchurch, New Zealand, 2016.

[4] G. Beattie, R. Shelton, S. Thurston and A. Liu. “The Performance of Residential Houses in the Darfield Earthquake of 4 September 2010”. In: the 9th Pacific Conference on Earthquake Engineering. Auckland, New Zealand, 2011.

[5] Z. Chen, Y.H. Chui, G. Doudak and A. Nott. “Contribution of Type-X Gypsum Wall Board to the Racking Performance of Light-Frame Wood Shear Walls”. In: Journal of Structural Engineering, 142.5 (2016), 4016008.

[6] K. Wang, M. Li, R. Dhaka, and A. Liu. “Comparison of Seismic Performance on Plasterboard Bracing Walls and Plywood Shear Walls in the Context of New Zealand Light Timber-Framed Structures”. In: Canadian Conference - Pacific Conference on Earthquake Engineering, Vancouver, British Columbia, 2023.

[7] Standards New Zealand. “NZS 3604:2011 Timber-Framed Buildings”. Standards New Zealand, Wellington, NZ, 2011.

[8] A. Liu and R. Shelton. “SR404 Seismic Effects of Structural Irregularity of Light Timber-Framed Buildings”. BRANZ, Judgeford, Wellington, 2018.

[9] Standards New Zealand. “ NZS 1170.5:2004 Structural Design Actions. Part 5: Earthquake Actions - New Zealand". Standards New Zealand, Wellington, NZ, 2004.

[10] M. Li, F. Lam, R. Foschi, S. Nakajima, and T. Nakagawa. “Seismic Performance of Post and Beam Timber Buildings I: Model Development and Verification”. In: Journal of Wood Science 58.1 (2012), pp. 20-30.

[11] R. Foschi. “Modelling the Hysteretic Response of Mechanical Connectors for Wood Structures”. In: the 6th World Conference of Timber Engineering, Whistler, Canada, 2000.

[12] M. Li, R. Foschi and F. Lam. “Modeling Hysteretic Behavior of Wood Shear Walls with a Protocol-Independent Nail Connection Algorithm”. Journal of Structural Engineering, 138.1 (2012), pp. 99–108.

[13] D. Moroder. “Floor diaphragms in multi-storey timber buildings”. PhD thesis. University of Canterbury, 2016.

[14] D. Vamvatsikos and C. Cornell. “Incremental dynamic analysis”. In: Earthquake engineering & structural dynamics, 31.3 (2002), pp. 491-514.

[15] D. Vamvatsikos, F. Jalayer and C. Cornell. “Application of incremental dynamic analysis to an RC-structure”. In: Proceedings of the FIB symposium on concrete structures in seismic regions, 2003.

[16] D. Vamvatsikos and C. Cornell. “Applied incremental dynamic analysis”. In: Earthquake spectra, 20.2 (2004), pp. 523-553.

[17] H. Naderpour and P. Fakharian. “A synthesis of peak picking method and wavelet packet transform for structural modal identification”. In: KSCE Journal of Civil Engineering, 20(2016), 2859-2867.

[18] S. Ivanovic, M. Trifunac and M. Todorovska. “Ambient vibration tests of structures-a review”. In: Journal of earthquake Technology, 37.4 (2000), pp. 165-197.

[19] G. Hafeez, A. Mustafa, G. Doudak and G. McClure. “Predicting the fundamental period of light-frame wood buildings”. In: Journal of Performance of Constructed Facilities, 28.6, (2014), A4014004.

[20] H. Aslani and E. Miranda. "Probability-based Seismic Response Analysis". In: Engineering Structures. 27,8 (2005), pp. 1151-1163.

[21] J. Mander, R. Dhakal, N. Mashiko and K. Solberg. "Incremental dynamic analysis applied to seismic financial risk assessment of bridges". In: Engineering Structures. 29,10 (2007), pp. 2662-2672.


https://doi.org/10.52202/080513-0176